Fall 2016

MAJOR FRACTION OF BLACK CARBON IS FLUSHED FROM NEW HAMPSHIRE SEASONAL SNOWPACK EARLY IN MELT

James Lazarcik
University of New Hampshire, Durham

MAJOR FRACTION OF BLACK CARBON IS FLUSHED FROM NEW HAMPSHIRE SEASONAL SNOWPACK EARLY IN MELT

BY

JAMES LAZARCIK

Bachelor of Science, Beloit College, 2013

THESIS

Submitted to the University of New Hampshire

In Partial Fulfillment of

The Requirements for the Degree of

Master

of

Earth Sciences: Geochemical Systems

September, 2016

This thesis has been examined and approved in partial fulfillment of the requirements for the degree Master's in Earth Sciences: Geochemical Systems by:

Thesis Director, Dr. Jack E Dibb
ESRC Director
Research Associate Professor of Earth Sciences

Dr. Cameron P Wake
Research Professor of Earth Sciences

Dr. Madeleine M Mineau
Research Assistant Professor of Earth Sciences

On June 20 2016

Original approval signatures are on file with the University of New Hampshire Graduate School.

ACKNOWLEDGEMENTS

Thanks Jack - for every opportunity you allowed me during my time here on the east coast, all of your help with editing, writing, and imparting your knowledge and enthusiasm of science to me. I have had a blast. Thanks Cam - for your help, suggestions, and guidance during this whole endeavor. Thanks Madeleine - for putting up with my relentless email barrages and continuing to provide great feedback, edits, and suggestions with all of my work. Other big thanks go to Alden Adolph, Jacki Amante, Eric Scheuer, and Mary Albert for their help in the lab and editing this work. Even more thanks go to Brian Taetzch, Megan Dalton, Jeferson Prado Swerts, Jessica Lindes Fonseca, and Tristan Amaral for the hours spent freezing on my behalf. Thanks to Taylor Hodgdon for assistance with figures and maps and Amanda Houts for help with figures and the many hours spent decompressing. Thanks to Sallie Whitlow and all of your critters for insightful conversations and making many of these days brighter than others. Thanks all the folks in the ESRC who have answered some of my endless questions. Thank you to Linda Kalnejais for helping me get into school in the first place. Thanks to Karrie and Steve Myer for being great role models. Ellie – thanks for all of your assistance, companionship, and putting up with me in general. Support for the New Hampshire EPSCoR Program is provided by the National Science Foundation's Research Infrastructure Improvement Award # EPS 1101-245.

TABLE OF CONTENTS

ACKNOWLEDGEMENTS iii

LIST OF TABLES vi

LIST OF FIGURES vii

ABSTRACT viii

CHAPTER PAGE

I. INTRODUCTION 1

II. METHODS 3

Site Locations 3

Sampling Summary 3

Snowpit Sampling 4

Analysis 4

BC Analysis Uncertainty 5

Data Processing 7

Impurity Inventory 7

Quality Control 7

Identifying periods of active melt 9

Concentration Factors 9

III. Results 11

Spatial Variability 11

Seasonal Overviews 11

First Fraction of Melt 13

Impurity Pulse 15

IV. DISCUSSION 17

Spatial Differences 17
Impurity Pulse 17
Prolonged Melt Impurity Dynamics 20
V. CONCLUSIONS 23
VI. RECOMMENDATIONS FOR FUTURE RESEARCH 24
REFERENCES CITED 37
APPENDIX 41

LIST OF TABLES

TABLE		PAGE
Table 1	Overview of sampling seasons	27
Table 2	Average coefficient of variation for seven NH surveys	27
Table 3	Median BC, Cl^-, NO_3^-, and sample density	28
Table 4	Maximum integrated SWE, integrated inventory and average concentration at maximum SWE	28
Table 5	Percent and absolute inventory changes during first fraction of SWE loss	29

LIST OF FIGURES

FIGURE		PAGE
Figure 1	Site locations for Winter 3	30
Figure 2	Inventory for Cl^-, NO_3^-, and BC during Winter 3 at BDO	31
Figure 3	Daily impurity loss during first melt fraction	32
Figure 4	Concentration factor of snowpack meltwater during March 2015 at BDO	33
Figure 5	Vertical redistribution of BC during first melt fraction at BDO in Winter 3	34
Figure 6	Concentration factor of snowpack meltwater during March 2015 at DFO	35
Figure 7	End of season BC and Cl^- surface concentrations at BDO during Winter 3	36

ABSTRACT

MAJOR FRACTION OF BLACK CARBON IS FLUSHED FROM NEW HAMPSHIRE SEASONAL SNOWPACK EARLY IN MELT

by

James Lazarcik

University of New Hampshire, September, 2016

Seasonal snowpacks accumulate soluble impurities derived from atmospheric aerosols and trace gases throughout the winter and release them quickly early during snow melt. Previous field and laboratory studies have shown that a snowpack can lose up to 80% of the ion burden in the first 20% of the melt, an event commonly known as an ionic pulse. Other studies have concluded that particulate impurities (e.g. black carbon (BC)) concentrate in surface layers during melt which can have important implications for snowpack albedo. To characterize snow chemistry, quantify the release of impurities, and qualify enhancement effects, we collected and analyzed near daily chemical profiles in the snowpack at three sites during two winters in New Hampshire, United States of America. We observe an ionic pulse of major ions and a pulse of BC from the snowpack at the onset of melt, with up to 62% of BC leaving with the first 24% of the melt. Surface concentrations of BC are higher than seasonal medians at the end of the winter season, but enhancements do not appear to be closely linked to decreases in snow-water equivalence.

I INTRODUCTION

Black carbon (BC) may be one of the most important individual contributors to climate warming [Hansen and Nazarenko, 2004; Bond et al., 2013]. Recent estimates for total radiative forcing by BC are as high as +0.40 W/m^2 (+0.05 to +0.80) [Myhre et al., 2013]. The presence of BC in and on snow and ice contributes approximately ten percent (+0.04 W/m^2 (+0.02 to +0.09)) of the total radiative forcing effect due to its high absorption of visible light [Bond et al., 2013; Myhre et al., 2013]. When BC is on the surface snow during times of melt, it has the potential to darken the snowpack and lead to positive albedo and grain size feedback loops. The effect of the both feedback loops is increased absorption of radiation causing acceleration of snow melt and grain growth, further decreasing snow albedo thereby decreasing snow cover duration and global surface albedo [Flanner et al., 2007; Doherty et al., 2013]. Thus, the behavior of BC in arctic, subarctic, and high-altitude snowpacks is an area of interest [Doherty et al., 2010; Doherty et al., 2013; Bond et al., 2013; Doherty et al., 2016]. However, there is little published field data regarding the behavior of BC in mid-latitude, low-altitude seasonal snowpacks during melt, though Doherty et al., [2014; 2016] extensively discuss mid-latitude BC in central North America and the mountains of Idaho and Utah, respectively.

Recent studies in melting snowpacks have found that BC amplifies on the surface of the snowpack [Meinander et al., 2013; Doherty et al., 2013], where a reduction of snowpack albedo due to increased grain size or BC concentrations could be significant [Flanner et al., 2007]. Other studies have shown a flushing of particles during melt [Conway et al., 1996], sometimes causing a 75% reduction in BC concentration [Sterle et al., 2013]. Studies that focus on melt accumulation or deposition of BC [Hansen and Nazarenko, 2004; Aamaas et al., 2011; Svensson et al., 2013; Tedesco et al., 2016] often cite Conway et al. [1996] in support of a melt accumulation or enhancement argument, even though Conway et al. showed that most hydrophobic soot still flushed through the snowpack with relatively high efficiency. A large BC

meltwater scavenging efficiency has the potential to significantly decrease the radiative forcing effect of BC in snow [Qian et al., 2014].

This study uses daily snowpit measurements to focus on changes in depth profiles and burden of BC during active melt in New Hampshire's (NH) seasonal snowpack. We also include measurements of major ions Cl^- and NO_3^- to validate our approach of estimating changes in impurity burden. Previous studies using lysimeters have shown that major ions pulse from the snowpack at the onset of melt [Johannessen et al., 1976; Johannessen and Henricksen, 1978; Hibberd, 1984; Williams and Melack, 1991; Bales et al., 1989; Harrington and Bales, 1998a, 1998b; Sotah et al., 1999; Feng et al., 2001; Lee et al., 2008; Williams et al., 2009]. Therefore, if daily integrated snowpit sampling allows us to detect a pulse of major ions, the same method should be applicable to BC melt dynamics. Since meltwater scavenging efficiency for BC is much lower than for major ions [Colbeck, 1981; Conway et al., 1996; Doherty et al., 2013], we expect a natural juxtaposition between major ion and BC melt dynamics.

The initial motivation for this study was to investigate the effects of BC evolution in the melting NH seasonal snowpack on albedo. An in depth analysis regarding BC, optical grain size, and albedo in the seasonal NH snowpack is provided in Adolph et al., [2016]. Adolph et al. [2016] find the albedo effect of BC in NH snow is secondary to grain size effects. However, observations of BC in melting snowpacks presented in this work may help lower uncertainty associated with treatment of BC in aging snow as it is implemented in snowpack models or modules [Flanner et al., 2007].

II METHODS

Site Locations

Physical and chemical snowpack properties were measured at three sites spanning the southern half of New Hampshire (Figure 1). Two sites were located near the University of New Hampshire, Durham, NH in New Hampshire's seacoast region, Burley-Demeritt Open Field (BDO, N 43°05', W 70°59', 35 m a.s.l.) and Thompson Farm Open Field (TFO, N 43°06', W 70°56', 19 m a.s.l.). A third site, Dartmouth Organic Farm Open Field (DFO, N 43°44', W 72°15', 119 m a.s.l.) was located on the border of New Hampshire and Vermont along the Connecticut River near Dartmouth College in Hanover, NH. The Hanover site was located at the Cold Regions Research and Engineering Lab Yard Open Field (CYO, N 43°43', W 72°16', 143 m a.s.l.) in the winter of 2013-2014. The site was moved to a nearby farm in the winter of 2014-2015 to be more similar to the open farm field sites established near the seacoast. Each field site consists of gently sloping or level terrain and is near meteorological stations, which collect relevant meteorological data throughout the winter.

Sampling Summary

Two sampling seasons are studied in this work, referred to as Winter 2 and Winter 3. A first winter (Winter 1) was a trial sampling season. Data for Winter 1 can be found at https://ddc.unh.edu/ddc_data/variables/list/. Sampling seasons vary in collection days and sampling frequency (Table 1); the target was to sample the snowpack daily. Winter 2 was a warmer winter season overall but Hanover saw its highest snowfall totals as well as its highest percentage of coastal/sea based storms [Adolph et al., 2016]. Winter 3 (the most complete sampling campaign) was a colder winter at all three sites. The seacoast saw its highest snowfall totals and Hanover received its highest percentage of land based storms. Adolph et al., provide more details pertaining to winter campaign meteorological trends and differences.

Snowpit Sampling

Field sampling involved multiple measurements in an area of previously undisturbed snow. A snowpit was dug and a planar wall created using a plastic shovel that was carefully cleaned daily with 18 MΩ RO water. Then, depth range and temperature in each identifiable snowpack layer were determined. Depth was characterized with a ruler. Albedo and grain size were also characterized, and Adolph et al. [2016] provide information regarding albedo and grain size sampling and analysis.

In Winter 3, snow samples of known volume and depth were collected at ambient temperature continuously from top to bottom with respect to snowpack layers. In Winter 2, samples were obtained at fixed depths without regard for snowpack layers. Samples were excavated using a 100 mL density cutter. In the field, samples were put in tared, pre-cleaned 175 mL HDPE bottles [Dibb et al., 2007]. Two side-by-side scoops at a depth resolution of 1 to 6 cm were placed into a single bottle. After collection, samples were stored in a cooler with sufficient thermal mass for transport back to the lab where they were weighed to determine sample density and snow-water equivalence (SWE). Samples were subsequently stored in a freezer at approximately -20 °C until analysis.

After a daily pit had been excavated and sampled, it was re-filled using the original snow. This helps mitigate the development of horizontal temperature gradients and stop flux of water vapor and atmospheric aerosols into and out of the full depth of the snowpack. Subsequent pits were typically located in an area of undisturbed snow 0.5 m south-east of the previous pit. Because each daily pit is in a slightly different location, meter scale spatial variability of impurities and SWE were also characterized through seven spatial surveys.

Analysis

Snow samples were melted in batches of five by standing the sample bottle in a room temperature water bath prior to analysis. Immediately after melting, each sample was sonicated

for at least 15 minutes then aliquoted to a smaller analysis bottle. First, snow water was analyzed for BC concentration via laser-induced incandescence on the single-particle soot photometer (SP2; Droplet Measurement Technologies). Liquid snow samples were aerosolized with an ultrasonic nebulizer (USN) (CETAC U5000AT) at a constant 1 SLPM air flow and 0.6 mL/min liquid sample introduction. The SP2 and nebulizer were both externally calibrated with fullerene soot [Schwarz et al., 2006]. After analysis on the SP2, samples are queued for major ion analysis (Na^+, NH_4^+, K^+, Mg^{2+}, Ca^{2+}, Cl^-, NO_3^-, SO_4^{2-}) via ion chromatography (IC) [Dibb et al., 2007], though Cl^- and NO_3^- are the primary major ion focus in this work.

BC Analysis Uncertainty

Analysis of BC can be complicated by a variety of factors, one of which is diameter dependent nebulizer efficiency. The U5000AT has greatly decreased efficiency for BC particles > 500 nm [Schwarz et al., 2012; Ohata et al., 2013; Wendl et al., 2014] and has been specifically advised against for snow analysis where BC diameters are expected to be > 500 nm [Schwarz et al., 2012]. Based on preliminary SP2 results from this study, BC mass concentration diameter modes should be within the most efficient range of the U5000AT, or about 100 nm to 500 nm [Ohata et al., 2013], and similar to fullerene soot standard diameters [Laborde et al., 2012; Wendl et al., 2014].

Dust may also externally mix with BC and effectively increase BC particle size. The SP2 is relatively insensitive to external dust/BC mixtures [Schwarz et al., 2012; Wendl et al., 2014], but the U5000AT may inefficiently aerosolize BC particle mixtures with a diameter of > 500 nm. A recent study concluded that even mid-latitude North American sites far from globally significant dust sources may have significant contributions of local dust and dirt present within the snowpack [Doherty et al., 2016], but relatively little dust is present in the NH snowpack. For either campaign in this study, the highest mean dust concentrations are about 1 ppm [Adolph et al., 2016] based on Ca^{2+} concentrations [Polashenski et al., 2015]. This represents a high upper

limit; Ca^{2+} is found in sea-salt aerosol and it is likely some winter-time Ca^{2+} is sourced from the treatment of roads with $CaCl_2$ during particularly cold periods. Schwarz et al., [2012] find a small positive offset in SP2 BC mass with high dust concentrations but very little associated size distribution shift.

Black carbon in snow is larger than found in the atmosphere and also may experience slight size distribution shift during melt/freeze cycles [Schwarz et al., 2013], though the evidence for this is sparse. Lab experiments demonstrate that freezing liquid standards can cause loss of BC mass when later thawed and reanalyzed [Kaspari et al., 2011; Schwarz et al., 2013] and hint that a small fraction of BC (< 5%) may agglomerate into larger particles [Schwarz et al., 2013]. However, a signal of less than 5% shift in size distribution is likely going to be lost in the error associated with analysis (± 25% for USN/SP2 [Ohata et al., 2013]; ± 27% average USN/SP2 standard deviation in this study). Furthermore, Schwarz et al., [2012] and Wendl et al., [2014] note that they do not observe a significant shift in mass size distribution in snow samples that experience melt/refreeze cycles.

Loss of BC mass to HDPE container walls is another potential source of uncertainty if a sample is stored at room temperature for 24 hours and later analyzed [Ogren et al., 1983; Schwarz et al., 2012]. However, HDPE bottles only result in less than 10% variability when compared to other bottle types (e.g. glass) for analysis following sonication [Wendl et al., 2014]. As long as samples are continuously frozen until analysis and sonicated just prior to analysis, as they were in this study, use of HDPE bottles should not significantly impact results [Wendl et al., 2014].

Data Processing

Impurity Inventory

Data from the IC and SP2 are reported as concentration in melted snow, with units of nmol/L and ng BC/g liquid (both hereby converted to ppbw), respectively. Inventories (i.e. impurity burden per unit area) were calculated on a sample by sample basis using Equation 1 (units in parentheses):

$$\mathrm{Inv_j}\left(\frac{\mathrm{ng}}{\mathrm{cm^2}}\right) = [\mathrm{j}]\left(\frac{\mathrm{nmol}}{\mathrm{L}}\right) \times \mathrm{M_j}\left(\frac{\mathrm{g}}{\mathrm{mol}}\right) \times \frac{1}{1000}\left(\frac{\mathrm{L}}{\mathrm{g\ liquid}}\right) \times \mathrm{SWE}\left(\frac{\mathrm{g\ liquid}}{\mathrm{cm^2}}\right) \qquad \text{Equation 1}$$

where j is a specific impurity contained in a single sample, [j] is impurity concentration, and SWE is the sample SWE, and M_j is the molar mass of each specific major ion. Because BC concentrations are already reported in ng/g, M_j and the conversion from L to g liquid are omitted. Note the density of meltwater is assigned 1000 g/L. All inventories are added over the whole-day profile to obtain daily integrated inventory to evaluate day-to-day impurity additions or losses.

Quality Control

The dataset from both winters includes more than 2900 snow samples extracted from ~ 440 pits (Table 1). Yearly dataset from each site are screened to determine outliers [Tukey, 1977]. Tukey defines an outlier filter in which extreme outliers, or data points that fail the below definition, are flagged for further examination.

$$[\mathrm{j}] < \mathrm{IQR_j} \times 1.65 + 3\mathrm{Q_j} \qquad \text{Equation 2}$$

IQR is the interquartile range for a site dataset, and 3Q is the value of the third quartile for a specific impurity. Tukey multiplies the IQR by the arbitrary value of 1.5 which we increase to 1.65 to include an approximation of 15% instrument error. This method is used to place bounds on a dataset and flag data points that are extreme deviations. Therefore, this metric is only used

to identify individual data points that seem anomalous in order to examine them further to determine their quality.

Generally, extreme outliers for most impurities occur in groups and can be plausibly explained by deposition of dust or other aerosols. For example, Na^+, Mg^{2+}, and Ca^{2+} outliers generally occur together in the same initial surface samples and can be traced for a period of time in subsequent snowpits. Therefore they are attributed to dust or mineral deposition events. Similarly, outliers for SO_4^{2-} and NO_3^- generally meet the same criteria as above, and can be attributed to acidic aerosol deposition. Samples that are flagged as extreme outliers and show no evidence of heightened concentration in the same storm layer in preceding or following snowpits are further scrutinized. In the end, samples that have outliers for K^+, Na^+, and Cl^- are removed on the grounds of contamination from the person sampling or handling the sample in the lab. One or two samples at greatest snowpit depth are usually orders of magnitude more concentrated in K^+ than samples dispersed throughout the rest of the snowpack. These are thought to be contaminated by the soil surface beneath the snowpack and are also removed. For all sites in Winters Two and Three, 1.8% and 1.1% of samples are rejected due to human contamination and 9.2% and 9.7% of samples are rejected due to soil contamination, respectively.

Samples that have been disqualified are not expected to greatly impact further analysis. Often, samples from the bottom of the snowpack have observations of debris or dirt in the sample indicating overzealous sampling resulting in extraordinary K^+ concentrations. Removing basal samples is equivalent to assuming that snow and impurities so close to the ground have left the snowpack. Samples that have been selectively removed due to human contamination are not thought to have much of an effect on the snowpack inventory calculated for any given pit as the number of samples per snowpit on these days is usually large (> 10). Overall, a single sample comprising of at most 6 cm total depth contributes less to the snowpack inventory than is possible from other sources of uncertainty.

Identifying periods of active melt

Rapid snowpack changes accompany the onset of melt; therefore, objective identification of the start and duration of active melt is of particular importance. A linear weighted-moving-average [Ulrich, 2015] of five consecutive days was applied to a full season of integrated SWE data to obtain a smoothed daily SWE profile. Smoothed SWE effectively removes spatial variability and allows for objective identification of downward trending SWE. Melt periods are considered to be active when the smoothed SWE profile decreases for at least three days in a row. The start day of the active melt cycle is then defined as the first day where a decrease in smoothed SWE was observed. The end of a melt cycle is when smoothed SWE trends up or the snowpack depletes completely. Many previous field and lab studies that investigate the generation of an ionic pulse have defined the first melt fraction to be after 20-30% SWE loss [Johannessen and Henriksen, 1978; Colbeck, 1981; Sotah et al., 1999; Williams et al., 2009]. In this study, measured SWE the day before melt began is defined as SWE at day zero (SWE_0) and the ratio of subsequent integrated SWE divided by SWE_0 is used to determine the first melt fraction, or when approximately 20%-30% SWE loss has occurred.

Concentration Factors

During times of active melt, we consider the most relevant physical process in the snowpack to be meltwater percolating down and out of the bottom of the snowpack. Therefore, any concurrent decrease in SWE and impurity inventory is interpreted as a release of water and impurities to the surrounding environment. Since impurity and SWE additions to the snowpack may occur with rain and snow events during times of melt, calculated loss is a lower limit for what is actually lost from the snowpack. Meltwater concentrations cannot be calculated in instances where SWE and impurity inventory do not decrease concurrently, though negative losses (impurity inventory gains) are calculated when inventory increases coincident with

decreasing SWE. The concentration of each impurity leaving the snowpack in meltwater is calculated with Equation 3:

$$[\mathrm{j}]_{\mathrm{meltwater}}\left(\frac{\mathrm{ng}}{\mathrm{g}}\right) = \Delta\mathrm{Inv_j}\left(\frac{\mathrm{ng}}{\mathrm{cm^2}}\right) \times \frac{1}{\Delta\mathrm{SWE}}\left(\frac{\mathrm{cm^2}}{\mathrm{g\ liquid}}\right) \qquad \text{Equation 3}$$

where $\Delta\mathrm{Inv_j}$ is the calculated integrated inventory change from one day to the next and ΔSWE is integrated SWE change from one day to the next. Calculated meltwater concentrations are in units of ng/g (ppbw). A small decrease in SWE accompanied by a decrease in impurity inventory will result in a large calculated meltwater concentration. This is a common finding in field and laboratory snowmelt studies that use lysimeters or snow columns to analyze major ions in meltwater. Calculated meltwater concentration divided by the average concentration in the snowpack at the beginning of melt yields a concentration factor (CF; unitless) [Johannessen and Henricksen, 1978].

III RESULTS

Spatial Variability

Spatial variability estimates aid in determining which snowpack chemistry changes reflect temporal changes as opposed to changes in chemistry due to sampling in a different location each day. Two to nine pits sampled in succession were studied on seven occasions throughout both sampling campaigns. Meter scale variability of Cl^- and NO_3^- observed in NH seasonal snow (Table 2) are similar to coefficients of variance (CV) reported for Greenland snow [Hart, 1997; Dibb and Jaffrezo, 1997]. Meter scale variability of BC in NH (Table 2) is also in accord with values for elemental carbon in surface snow of Arctic Finland reported by Svensson et al. [2013] and values reported in Doherty et al. [2010, 2014, 2016]. The variability of SWE at our study sites (Table 2) is lower than the average SWE variability for six Greenland surveys reported in Hart [1997].

Seasonal Overviews

Since concentrations cannot be less than zero, natural snow data trends to a positive skew. Thus, the median is the best measurement of central tendency for inter-site and inter-study comparison. Median Cl^- concentration in Hanover during Winter 3 is about 400% higher than median seacoast Cl^- concentrations, while median NO_3^- concentrations across the state are similar (Table 3). Given that sea-salt aerosol deposition rapidly decreases with distance from the coastline [Gustafsson and Franzén, 1999; Liang et al., 2016], there appears to be a strong source of non-sea-salt Cl^- in Hanover in Winter 3.

Median Cl^- concentration in Hanover during Winter 2 is only slightly higher than near the seacoast (Table 3), while NO_3^- concentration in Hanover is about 150% higher than near the seacoast. Overall, Cl^- and NO_3^- concentrations in NH are much lower than Cl^- [Oliver et al., 1974] and NO_3^- [Bock and Jacobi, 2010] concentrations reported for urban snow collected from

rooftops, but much higher than median concentrations reported for remote Greenland [Dibb et al., 2007].

Median BC concentrations in Hanover are always higher than concentrations on the seacoast (Table 3), with Hanover receiving about 15% more concentrated BC in Winter 3, and 60% more concentrated BC in Winter 2. Overall, median BC concentrations in NH snow are similar to mean concentrations reported for remote Sierra Nevada sites [Hadley et al., 2010] and some Arctic sites [Doherty et al., 2010], and higher than mean concentrations reported for remote sites in Greenland [Polashenski et al., 2015]. In contrast, BC concentrations at sites with similar elevation and latitude in the Northern U.S. Plains [Doherty et al., 2014] are typically much higher than BC concentrations in NH. However, seasonal median concentration are not the best comparison to Doherty et al., [2014] as they tried to sample at near max SWE before melt.

Major ions and BC at maximum SWE (Table 4) reflect the main site and campaign differences outlined in the description accompanying Table 3, which indicates that observations of impurity concentrations during SWE maximum can be representative of a region in some cases. Note that BC concentrations reflect differences noted in Table 3, while the inventory near the seacoast during Winter 3 is comparable to BC in Hanover. This is because Hanover received less snow, which leads to a higher concentration. In contrast, average BC concentration at max SWE in Hanover during Winter 2 is 300%-500% greater than the seacoast despite Hanover having 200% more snow at max SWE (Table 4). This may be caused by the temporal difference in max SWE at each location, so some caution needs to be kept in mind when a single pit is assumed to represent a site more generally than just on the day a sample was obtained.

Integrated SWE from Doherty et al., [2014] is comparable to seasonal maximum SWE in NH; however, integrated BC in NH (Table 4) is typically much lower than estimates of integrated BC in central North America when the amount of snow water is taken into account.

Average BC concentration at SWE max in NH (Table 4) is generally far less than average BC mixing ratios listed Doherty et al., [2014].

Time series analysis of each pit during Winter 3 at BDO, which is the most comprehensive dataset, reveals snow layers with distinct impurity inventories that persist through most of the winter (Figure 2). Air temperature at BDO during the month of February was low enough that the snowpack did not undergo noticeable diurnal melting and freezing, thus no ice layers were recorded in the snowpack until early March. There were additions of all three impurities to the surface of the snowpack following a major snowfall on the 28th of January. The impurities remain at the surface of the snowpack for a few days as the fresh snow begins to densify, but they are covered by the next snowfall event on the 2nd of February. Buried impurity layers remain discernable throughout the majority of the winter; they are further buried by later snowfall and approach the underlying surface due to densification, until the onset of melt in March (Figure 2). Generally, water equivalent depth of each distinguishable snowpack layer did not change from deposition until melt in March (not shown). Other impurity layers (e.g. impurities introduced with the snowfall on February 5th and 15th) occur throughout the winter and also remain discernable until the March melt period, when the discrete stratigraphic layers of snow become less distinct.

First Fraction of Melt

The snowpack accumulates impurities throughout the season (Figure 2) and releases them in meltwater during an active melt period. The first melt fractions were objectively determined (see section 2.5.3) and impurity inventories traced at each site during Winters 2 and 3. In order to put changes in inventory into context with changes in SWE, ΔInv for BC, Cl^-, and NO_3^- are plotted vs. ΔSWE (Figure 3). Every change in ΔInv and ΔSWE is relative to their respective values at the corresponding SWE_0.

In Winter 3, Cl^- and NO_3^- inventories continually decrease at a quicker rate than SWE (Figure 3c and 3e). This result is expected given the wide body of literature on the ionic pulse [Johannessen et al., 1976; Johannessen and Henricksen, 1978; Hibberd, 1984; Williams and Melack, 1991; Bales et al., 1989; Harrington and Bales, 1998a, 1998b; Sotah et al., 1999; Feng et al., 2001; Lee et al., 2008; Williams et al., 2009]. There are a few exceptions (i.e. points above the 1:-1 line), which is indicative of impurity inventory gain during melt. However, most major ion inventory losses in Winter 3 fall below the 1:-1 line, indicating a high major ion meltwater scavenging efficiency.

In Winter 2, major ion inventories still decrease quicker than SWE (Figure 3d and 3f), but not with the same clarity as in Winter 3. There are noticeable impurity inventory gains to the melting snowpack. Specifically, Cl^- in Hanover has high fractional gains during melt, but this may be due to the location of CYO relative to the CRREL parking lot (see Figure 1 in Adolph et al., [2016]). Otherwise, NO_3^- has some high fractional gains near the seacoast sites, but this may be an artefact of incomplete snowpack sampling or low temporal resolution with respect to Winter 3 (Table 1).

It is surprising, given that BC has a lower meltwater scavenging efficiency than major ions [Colbeck, 1981; Conway et al., 1996; Doherty et al., 2013], many BC inventory losses plot beneath the 1:-1 line in both Winters 3 (Figure 3a) and 2 (Figure 3b). There are some BC inventory gains during melt, which in Winter 3 can plausibly be caused by deposition to a thin snowpack. Deposition of BC to a snowpack with relatively low BC inventory will cause a large positive fractional inventory change. This may also be the case in Winter 2, but sampling inconsistencies (Table 1) could also be a factor.

Fractional inventory changes during Winter 3 indicate that major ions and BC share similar properties during the first melt fraction. This means that some snowpack BC in NH is

efficiently scavenged by meltwater. Observations of BC loss in the melting NH snowpack are supported by observations of hydrophilic and hydrophobic soot loss in a snowpack at Snowdome where over 50% of hydrophobic soot was flushed through the snowpack over the course of 10 days [Conway et al., 1996].

Impurity Pulse

The first melt fraction and total SWE and impurity inventory changes also indicate that BC is lost with comparable efficiency to major ions in some cases (Table 5). Each date range listed corresponds to a first melt fraction. Every early March inventory loss in Winter 3 is disproportionate to the amount of SWE lost, with most impurity inventories decreasing by over 40% with 20% SWE loss (Table 5). Considering all cases in Winter 3, inventory decreases quicker than SWE in 6 of 9 cases for Cl^-, 7 of 9 cases for NO_3^-, and 7 of 9 cases for BC.

Disproportional inventory losses in Winter 2 happen in only 5 of 11 cases for Cl^-, 7 of 11 cases for NO_3^-, and 2 of 9 cases for BC. The snowpack in Winter 2 more inventory changes of a smaller magnitude (Table 5), which leads to a lower signal to noise ratio and larger uncertainty. Additionally, the Winter 2 dataset has notable shortcomings - primarily missed sampling days (Table 1) and sporadic incomplete snowpack sampling, which may account for positive major ion inventory changes. Important to note, The Winter 2 dataset is not of sufficient quality to calculate CF time series.

Concentration factor time series during the last two melt events at BDO during Winter 3 (Figure 4) share some similar features of laboratory experiments detailing a solute pulse e.g. the highest calculated meltwater concentration is on the first day of melt [Johannessen and Henriksen, 1978; Colbeck, 1981; Bales et al., 1989]. Concentration factors for Cl^- and NO_3^- in each event are initially so large because of the relatively small amount of water and large amount of impurity inventory that left the snowpack. As the melt continues, CF for every impurity drops to or below 1.0. The peak calculated meltwater concentrations are 3.7 and 3.3 ppmw for

nitrate and chloride, respectively, in the first event, and 3.5 and 1.4 ppmw for the second event. BC has peak calculated meltwater concentrations of 18 and 22 ppbw for the same two March events.

IV DISCUSSION

Spatial Differences

Differences in median concentrations across NH were not always as anticipated, and may reflect different sources or modes of transport. In particular, the enhanced deposition of Cl^- in Hanover was not expected (Table 3). This is counterintuitive if the main source of Cl^- is sea-salt aerosol. Short range transport of road deicing agents may impact the snow chemistry in Hanover [Lundmark and Olofsson, 2007] and increased numbers of diesel vehicles may influence BC deposition [US EPA, 2009]. Adolph et al. [2016] show that Hanover typically encounters more storms originating over land to the west, whereas the seacoast encounters more coastal or sea based storms. Storm track differences or differences in impurity sourcing may also be contributing to differing impurity concentrations across NH. Wood burning stoves for heating may lead to increased BC concentration in snow as well. Up to 30% of homes primarily burn wood for heat in Grafton County (Hanover) compared to 0.1 – 5.0% in Strafford County (seacoast) [Finamore, 2013]. The origin of the airmass that eventually precipitates and proximity to I-91 may increase Cl^- concentrations, and the abundance of wood burning may additionally contribute to the increased BC we see in snow in Hanover.

Impurity Pulse

The behavior of BC during the first melt fraction is similar to the traditional ionic pulse measured in snowmelt. At BDO in Winter 3, the shape of the BC CF curve roughly mimics those for major ions from Mar 3 to Mar 17 but is very similar from Mar 24 to Apr 4, indicating that BC is washed from the snowpack in a similar manner to both chloride and nitrate (Figure 4). We do not quantify the specific chemistry of BC particles, but it is possible some BC particles have hydrophilic components or coatings, which could facilitate their transport by meltwater percolating from the surface of the snowpack.

Conway et al., [1996] found hydrophobic and hydrophilic soot applied to the surface of the snowpack behave quite differently during times of melt. In Conway et al., [1996], hydrophobic soot migrated into and through the snowpack, with just over 50% of soot applied in a 2.5 cm surface layer migrating out of the bottom of the pack. The remainder was retained within 28 cm of the surface. Hydrophilic soot, however, was almost entirely flushed from the snowpack, with just 1% of the initial application in the top 2.5 cm retained in the snowpack [Conway et al., 1996]. In the present study, 59% of BC mass at BDO in Winter 3 is lost with the ion pulse during the first March melt, while analysis of BC inventory distribution within the snowpack indicates the fraction of remaining BC mass migrates into lower snowpack layers (Figure 5). Colbeck, [1981] described a similar phenomenon for a snowpack doped with sodium chloride at various depths, where impurities migrate and concentrate at lower depths prior to leaving the snowpack later with melt.

The BC pulse in Hanover is larger than observed near the seacoast sites (Figure 6), and may be due to storm trajectories. Hanover receives more land based storms during the winter and also receives snowfall from air masses that have longer aerosol trajectory times [Adolph et al., 2016]. Longer aerosol transport times suggest Hanover receives BC that has had more time to react with strong oxidizing agents in the atmosphere (e.g. ozone) thus functionalizing the surface [Sergides et al., 1987]. Longer aerosol transport times could also lead to a decrease in BC size distribution as heavier particles are more likely to drop out [Liang et al., 2016]. The BC pulse in Hanover results in a maximum CF about 2-3 times greater than those seen at BDO in Winter 3 (Figure 6; see Figure 4 for comparison), which indicates more BC is mobilized by a smaller amount of meltwater in the DFO snowpack. Nitrate and chloride appear to flush out late in comparison to BC due to no continuous calculated major ion loss for that period (Figure 6). This is a combined result of spatial variability within the snowpack and SWE/impurity additions to the surface of the snowpack in exceedance of losses during melt.

The maximum CF for BC occurs about seven days after the start of active melt at DFO. After the eighth day, the BC CF drops to near 1.0, indicating a change in the effectiveness or rate of BC flushing. The abrupt change in effectiveness of BC loss at DFO in Winter 3 around day seven of active melt indicate that at least two large categorical fractions exist in the DFO snowpack: one fraction that flushes readily with small amounts of melt water (approximately 44% BC loss with 22% SWE loss for DFO in Winter 3 (Table 5)), and a second fraction that is flushed less readily or remains behind (the remaining 56% BC inventory). Major ions also show a decrease in effective loss, but this has previously been attributed to exclusion of most soluble species as snow grains age and varying grain scale distributions [Colbeck, 1981; Bales et al., 1989; Kuhn, 2001]. It is possible that BC is also excluded from grain surfaces during snow ageing, but this has not been tested or experimentally verified.

Because some BC tends to leave the snowpack at a faster rate than SWE during the first melt fraction (Figure 3) and BC losses can be large (Table 5), the percolating meltwater must be efficiently scavenging at least fraction of total snowpack BC. The reason BC in the NH snowpack has a higher affinity for percolating meltwater than ice crystals or other insoluble impurities in the snowpack is not known, but could involve hydrophilic BC surfaces/coatings and/or removal of a smaller diameter fraction. BC number and mass distribution modes during the five day January melt at DFO in Winter 3 (62% BC mass loss; 41% SWE loss (Table 5)) reveal no substantial change in particle diameter in the surface layer or overall snowpack. The surface BC number concentration mode increased from 75 nm to 85 nm while the surface BC mass concentration mode decreased from 220 nm to 200 nm. Neither change is statistically significant given uncertainty. The number concentration mode for this case is only slightly larger than the soot used by Conway et al. [1996] (60 nm for hydrophobic soot; data for hydrophilic soot not given) in their controlled study. The evidence presented above along with evidence of storm aerosol origin and transport presented in Adolph et al., [2016] suggest that BC particle

coatings or functionalization is the main contributor to the behavior of BC in NH snow, though further research on NH snowpack BC particle coatings and particle size is needed to confirm.

Prolonged melt impurity dynamics

Many studies focus on the melt amplification of surface BC during times of SWE loss from the snowpack, either through melt, sublimation, or dry deposition [Hansen and Nazarenko, 2004; Doherty et al., 2010; Aamaas et al., 2011; Doherty et al., 2013; Svensson et al., 2013; Tedesco et al., 2016]. Large increases in NH BC concentration during snow water loss would be consistent with melt amplification, but close examination of BC surface concentrations, SWE, and relevant meteorological observations (Figure 7) indicate that enhanced BC concentrations are not simply due to water loss or dry deposition in the NH snowpack. While surface BC concentrations are not at their absolute highest at the end of the season in this case, they are higher than the seasonal median (Table 2) and appear to be trending upward at times. Comparatively, surface Cl^- is consistently decreasing to the lowest concentrations for the season (Figure 7).

March at BDO in Winter 3 begins with relatively low surface BC concentration, which rapidly increases by over a factor of 4 during a 4% total SWE decrease (Figure 7). Even though SWE is going down, and from Mar 3 to Mar 4 total BC inventory is calculated as decreasing (Figure 5), this particular increase in surface BC concentration looks to be a result of a snowfall event. Between Mar 4 and Mar 5, surface BC concentration also increases. This event could plausibly be due to dry deposition (no snowfall recorded) and is in concordance with a slight increase in SWE, which may be due to spatial variability. Afterward, surface BC concentration decreases steadily until Mar 8 but remains constant through the period Mar 8 to Mar 9, where total BC inventory losses are again calculated (Figure 5). Mar 10 to Mar 11 is marked by a decrease in surface BC concentrations likely due to rain, while Mar 11 to Mar 12 is marked by a large concentration increase plausibly due to wind redistribution of the surface snow (Figure 7).

However, both days between Mar 10 and Mar 12 have total BC and SWE losses (Figure 5). The rest of the seasons end is marked by sporadic wind, rain, and snow events, all of which likely influence surface BC concentrations. Overall, there are only two 24 hour periods (Mar 15 to Mar 16; Mar 23 to Mar 24) where SWE decreases (indicating snowpack melt) and surface BC concentrations increase without confounding meteorological factors.

Doherty et al. [2013] describe a melt amplification of BC on the surface snow in Greenland at Dye 2 during times of melt due to inefficient meltwater scavenging. Our observations of BC behavior during melt in NH and subsequent hypotheses suggest that BC transported to central Greenland should be more hydrophilic, thus scavenged more efficiently. The Dye 2 snowpack experiences much colder temperatures than the NH snowpack and is over 2000 m higher above sea level than sites in this study. Consequently, Dye 2 accumulates much drier and colder snow, which likely leads to smaller individual snow grains and pore spaces as well as a slower rate of metamorphism. At Dye 2 the average density for the surface down to 60 cm depth was 0.42 g/cm^3 [Doherty et al., 2013]. The density of individual snow samples in NH rarely exceed 0.40 g/cm^3 and the few samples this dense are typically aged and located near the bottom of the snowpack. Densities of the surface layers during the first March melt hover around 0.20 g/cm^3; the median densities in NH do not exceed 0.27 g/cm^3 (Table 3). Colbeck [1979] describe a numerical model where meltwater percolation rate is inversely related to density and positively related to grain size, which may be factors leading to a mechanical restriction of insoluble particles, inhibiting depth migration. However, high latitude snowpacks generally melt much slower than lower latitude snowpacks [Qian et al., 2014] which suggests melt amplification may be dependent on the magnitude of snowpack melt.

There are other mechanisms by which BC could enhance on the surface of the snowpack other than insufficient meltwater scavenging. Evaporation and sublimation of water and snow on the surface of the snowpack [Box and Steffen, 2001] could lead to considerable BC enhancement, while ablation of snow can reveal underlying ice layers that were once

meltwater laden with BC [Tedesco et al., 2016]. In fact, Tedesco et al. [2016] suggest that the amplification of BC previously observed in the wet snow zone on the periphery of the Greenland ice sheet is mainly due to the processes mentioned above.

V CONCLUSIONS

This study provides extensive measurements of BC in the melting NH snowpack. We observe both similarities and differences between dynamics of major ions and BC during times of active melt. In the first melt fraction, Cl^-, NO_3^-, and BC are all lost from the snowpack at a quicker rate than SWE (Figure 3). The NH snowpack loses a maximum of 84% nitrate in 51% SWE loss, 95% chloride in 34% SWE loss, and 62% BC in 24% SWE loss (Table 5). Even BC is initially efficiently scavenged by meltwater in the NH snowpack, similar to the phenomenon described by Conway et al., [1996] for both hydrophilic and hydrophobic soot doped snow experiments in seasonal snow.

Black carbon also pulses from the snowpack in the same manner as major ions, with the highest meltwater concentrations calculated one to seven days after the start of active melt (Figure 4 and Figure 6). The affinity of BC for meltwater is likely due to functionalized BC surfaces or small BC particle diameter. However, size distribution analysis reveals that no significant change in particle size occurs during melt which suggests functionalized BC surfaces play a larger role in BC dynamics observed in this study. Surface BC concentration analysis at the end of the winter season show sparse evidence for melt amplification previously described [Meinander et al., 2013; Doherty et al., 2013], and suggests that local meteorological factors and rate of snowpack melt play important roles in NH surface BC concentrations at the end of the winter season.

VI RECOMMENDATIONS FOR FUTURE RESEARCH

This work has shown that BC dynamics in the NH seasonal snowpack can vary from observations of BC dynamics in alpine, arctic, and subarctic snowpacks. However, this work is based on data collected from three sites in NH; BC may not behave in the same manner in other low-altitude, mid-latitude seasonal snowpacks, primarily snowpacks that are further from the coast or snowpacks that receive aerosols sourced from different regions of the country. For example it would be useful to apply the same analysis to snowpacks in the Midwestern United States in order to deduce what effect proximity to the ocean and different aerosol transit times may or may not have on BC dynamics in seasonal snow. In addition, laboratory studies involving BC exposed to incremental concentrations of ozone for predetermined periods of time would also yield more information on the effect of transit time on BC oxidation.

Further work should be done on the specific chemistry of BC particles in NH. In order to analyze the snowpack for BC or major ions, the snow sample must first be melted, then sonicated, and in the case of BC analysis on the SP2, eventually nebulized, which destroys any higher order structure within BC aggregates and any specific BC coating. One potential solution to this problem would be to deploy an SP2 *in situ* and sample BC aerosol in atmospheric samples in the field in real time, bypassing the need to prepare snow samples for BC analysis. Not only would this allow for a determination of specific BC coatings and unaltered BC mass ranges, it would allow for a comparison to be made between BC properties measured just prior to deposition and BC measured during SP2 analysis of snow samples in the lab.

A curious observation that arose during analysis is that Hanover has about twice as much chloride load in any given winter compared to seacoast sites, despite being much further (130 km) from the ocean. It would seem that Hanover has an additional source of chloride in its snowpack and additional work should be done in order to pinpoint possible sources of chloride in Hanover snow. One potential source of chloride in the Hanover snowpack is the nearby roads

(which is one third the distance from DFO compared to the two seacoast sites), proximity to the interstate, or other nearby impervious surfaces. Halite from impervious surface treatment can be transported various ways to the snowpack, though most research suggests transport distance is minimal (less than 30 m from the road). However, there is some literature to suggest long range transport of deicing salts up to 1 km. Gradient grid surveys from nearby roads to applicable sample sites should be performed using the density cutter to sample at least the top storm layer of the snowpack following a deicing event in order to ascertain the effect of nearby roads on deicing salt burden in the snowpack.

Any further research on the pulse of major ions or BC in the NH seasonal snowpack during melt should involve measurements of the actual meltwater in addition to back-calculating meltwater concentrations based on day-to-day differences in snowpack inventory. Installing either a table top lysimeter and/or an in ground lysimeter may increase the accuracy of a pulse measurement, as the physical meltwater would not be subject to complex snowpack post deposition processes such as dry deposition, sublimation, resuspension, or wind-pumping. However, meltwater collection comes with its own set of potential problems to consider. Primarily, the lysimeter collection area must be large enough to accurately represent the collection site and care must be taken to account for preferred flow channels the snowpack may develop during times of melt. Further considerations would be ensuring the samples are not contaminated during collection and storage as well as keeping the collection line from freezing during particularly cold days, which are common in a typical NH winter.

In order to determine the potential ecological effects of meltwater entering a receiving ecosystem such as a stream, mass-balance calculations for each system should be performed. Meltwater sourced from the snowpack has an influence on the watershed in which the snow is deposited and effects of snowmelt can be measured in nearby streams, though it is currently unknown how the meltwater signal changes as it travels from the snowpack into the soil and stream systems. By calculating the mass of impurity leaving the snowpack and comparing it to

the mass of impurity flowing in the stream during a time of interest, a measure of how a meltwater signal changes while it travels to a stream can be deduced.

It should be noted that wherever complete time series records are pivotal for analysis, such as in determination of meltwater concentration factor, intensive measurements of greater than 15 cm snowpack depth are important. When the snowpack is below 15 cm depth, quality control protocol may disqualify up to 50% of the daily data based on contamination from the ground, which makes day-to-day interpretation more difficult. If a day-to-day record is not obtained through intensive sampling, linear interpolation over days missed makes interpretation of real day-to-day changes more difficult. Furthermore, if sections of a snowpit are periodically left un-sampled such as they were for sections of the winter two data set used in this thesis, a spurious variability is introduced which also skews interpretation of actual snowpack changes. Consequently, if studies analogous to the present one are to be performed, it is best to conduct them during a winter where field technicians have adequate time and adequate snow with which to work.

Table 1. Overview of sampling seasons

Site	Sampling window	Fraction of days sampled in window[a]	Total number of samples
	Winter 3: 2015		
DFO	Jan 1 – Apr 4	81/93	604
BDO	Jan 9 – Apr 4	77/85	555
TFO	Jan 9 – Apr 4	76/85	558
	Winter 2: 2013-2014		
CYO[b]	Dec 18 – Apr 10	76/113	491
BDO	Dec 18 – Mar 20	62/92	312
TFO	Dec 17 – Mar 28	73/101	390

[a]Number of sampled snowpits over possible number of pits
[b]CYO moved north-east to a nearby field (DFO) in Winter 3

Table 2. Average coefficient of variation for seven NH surveys[a]

	SWE	Cl^-	NO_3^-	BC
CV (%)	8.7 ± 4.2	27 ± 6.9	24 ± 4.2	42 ±17

[a]Coefficient of variance are shown as plus/minus standard deviation

Table 3. Median BC, Cl^-, NO_3^-[a], and sample density

Winter/ Site	BC (ppbw)	Cl^- (ppbw)	NO_3^- (ppbw)	Density (g/cm^3)
Winter 3				
DFO	5.60	563	514	0.27
BDO	3.90	129	415	0.24
TFO	4.20	163	461	0.25
Winter 2				
CYO	11.0	185	420	0.23
BDO	6.67	151	240	0.24
TFO	6.61	144	270	0.25

[a]Median concentrations are calculated over a full season of individual sample data after quality control

Table 4. Maximum integrated SWE, integrated inventory and average concentration[a] at maximum SWE

Winter/ Site	Date	SWE (g/cm^2)	BC ng/cm^2 (ppbw)	Cl^- ng/cm^2 (ppbw)	NO_3^- ng/cm^2 (ppbw)
Winter 3					
DFO	Mar 3	11.10	71 (6.4)	13100 (1180)	11400 (1030)
BDO	Feb 22	14.89	69 (4.6)	5210 (350)	10700 (719)
TFO	Mar 5	16.09	75 (4.7)	6880 (429)	12800 (794)
Winter 2					
CYO	Mar 13	14.37	350 (24)	3580 (249)	8000 (557)
BDO	Feb 21	6.99	54 (7.7)	1110 (158)	1930 (275)
TFO	Feb 22	7.90	34 (4.3)	762 (96.4)	1440 (182)

[a]Average snowpack concentration is calculated with integrated inventory and maximum integrated SWE similar to Equation 3.

Table 5. Percent and absolute inventory changes during first fraction of SWE loss[a]

	SWE %	Δ Inv g/cm^2	Cl^- %	Δ Inv ng/cm^2	NO_3^- %	Δ Inv ng/cm^2	BC %	Δ Inv ng/ cm^2
Winter 3					*DFO*			
Jan 22-26	41 ± 6	2.02	-31 ± 56	537	23 ± 30	174	62 ± 19	21.1
Mar 03-13	22 ± 8	2.43	62 ± 16	8120	64 ± 14	7350	44 ± 27	31.0
Mar 23-26	49 ± 5	5.05	46 ± 23	2520	65 ± 14	3530	18 ± 38	9.40
					BDO			
Jan 16-19	34 ± 7	0.55	95 ± 2	766	79 ± 8	429	-130 ± 120	2.88
Mar 03-11	27 ± 7	3.61	64 ± 15	3560	48 ± 21	5550	59 ± 21	42.3
Mar 23-27	51 ± 5	4.86	85 ± 6	755	84 ± 6	1720	57 ± 21	13.5
					TFO			
Jan 17-18	24 ± 8	0.42	58 ± 18	115	69 ± 12	709	62 ± 22	7.23
Mar 05-10	17 ± 8	2.79	49 ± 22	3350	29 ± 28	3740	34 ± 34	25.2
Mar 23-25	15 ± 8	1.23	-15 ± 49	178	-3 ± 41	107	46 ± 25	34.3
Winter 2					*CYO*			
Jan 06-10	26 ± 8	1.03	19 ± 35	142	23 ± 30	288	5 ± 44	1.99
Jan 21-27	35 ± 6	1.07	-150 ± 100	754	4 ± 38	103	-2 ± 46	0.74
Mar 03-09	9 ± 9	0.44	3 ± 41	71.6	14 ± 34	492	-81 ± 84	30.1
Mar 21-27	17 ± 8	2.13	-170 ± 120	3020	20 ± 32	1960	7 ± 41	18.9
Apr 01-04	36 ± 6	3.82	35 ± 28	1100	37 ± 25	1200	27 ± 32	54.3
					BDO			
Jan 06-07	42 ± 6	2.01	58 ± 18	691	69 ± 12	981	-36 ± 62	11.0
Feb 22-24	49 ± 5	3.06	67 ± 14	620	76 ± 10	1040	63 ± 19	27.3
Mar 07-12	43 ± 6	2.47	69 ± 13	1050	69 ± 12	1500	-4 ± 46	2.49
					TFO			
Jan 06-08	43 ± 6	1.95	30 ± 30	138	-54 ± 61	96.7	8 ± 55	0.73
Jan 26-30	36 ± 6	0.65	48 ± 22	601	59 ± 16	490	39 ± 28	6.24
Mar 10-14	26 ± 7	2.01	43 ± 24	748	37 ± 25	1070	-340 ± 200	72.6

[a]Percent uncertainty adjacent to percent change is spatial variability and instrument error

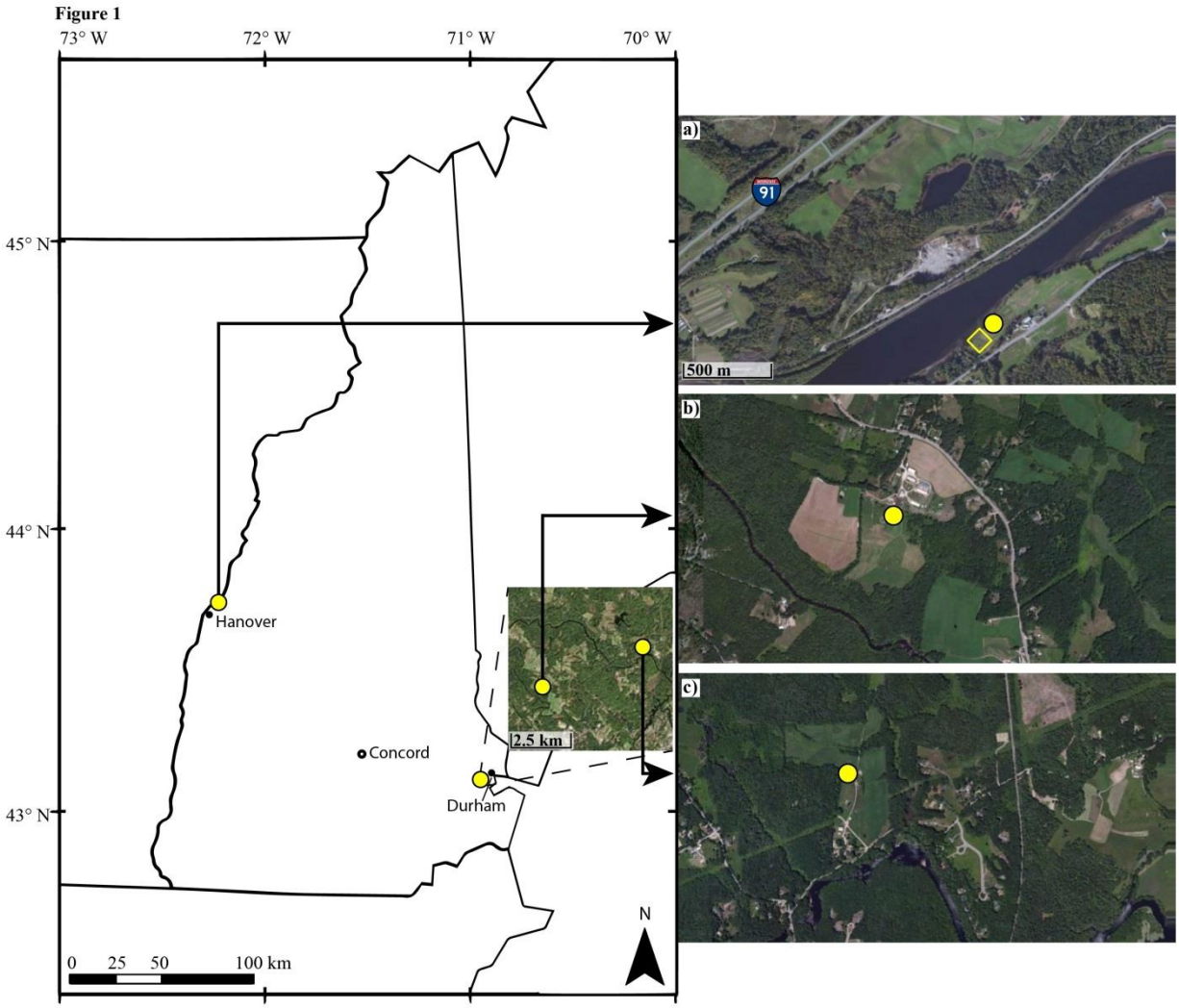

Figure 1. Site locations for Winter 3. DFO (a) on the western edge of New Hampshire in Hanover is near I-91 on the Connecticut River. BDO (b) and TFO (c) on the seacoast are located in Lee, NH and Durham, NH, respectively. The yellow square in panel a) is the approximate location of three separate surveys where samples were taken for spatial variability analysis.

Figure 2.

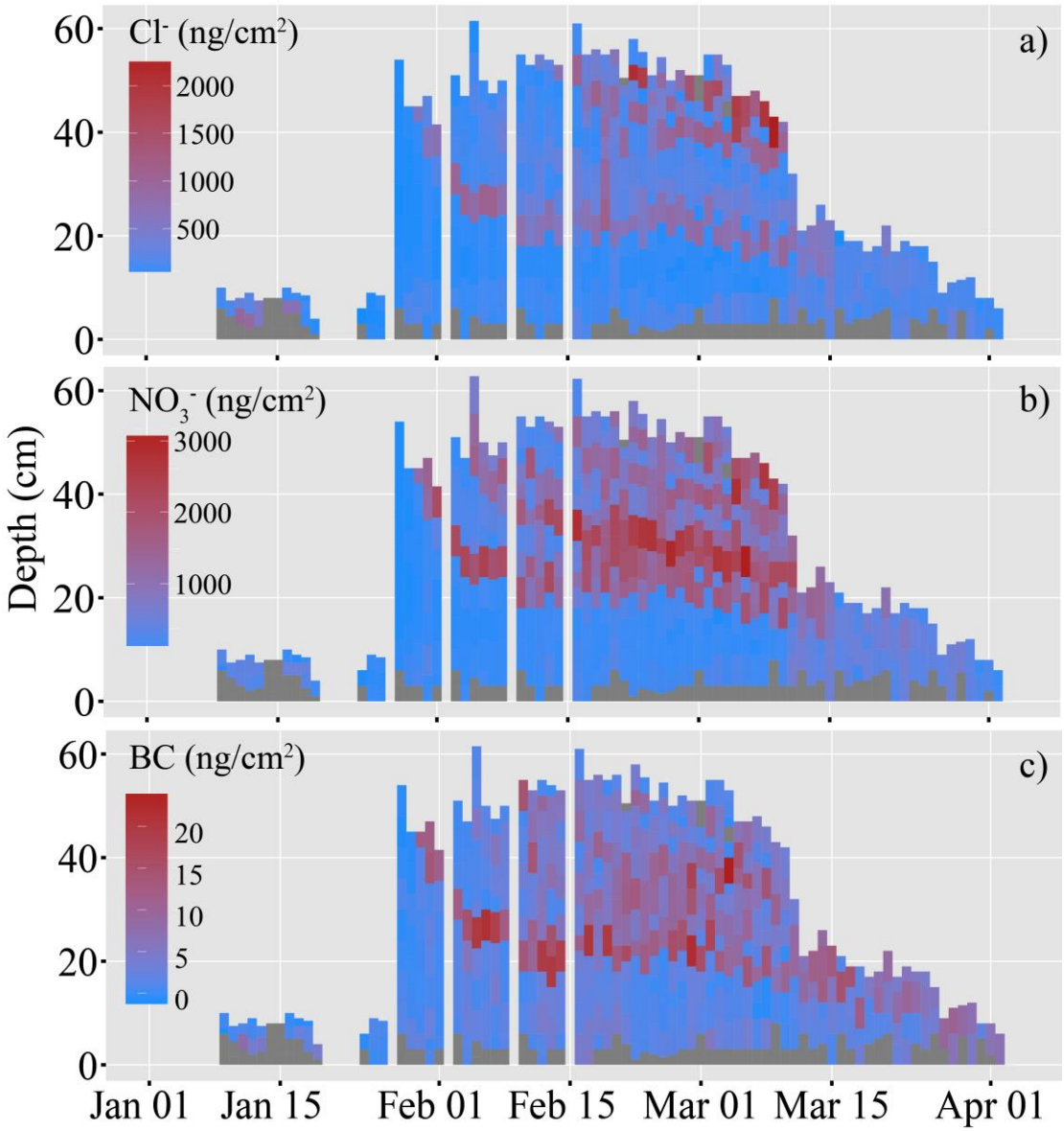

Figure 2. Inventory (relative amounts denoted with color) for Cl^- (a), NO_3^- (b), and BC (c), plotted against sample depth during Winter Three at BDO. The days with no inventory data in the middle of January are days where the snowpack completely melted, whereas the four days from the end of January to the middle of February are days where heavy snowfall prevented sampling. Each dark shaded box (typically near the bottom of the snowpack) represents samples that have been removed according to the QC protocol outlined in 2.5.2.

Figure 3.

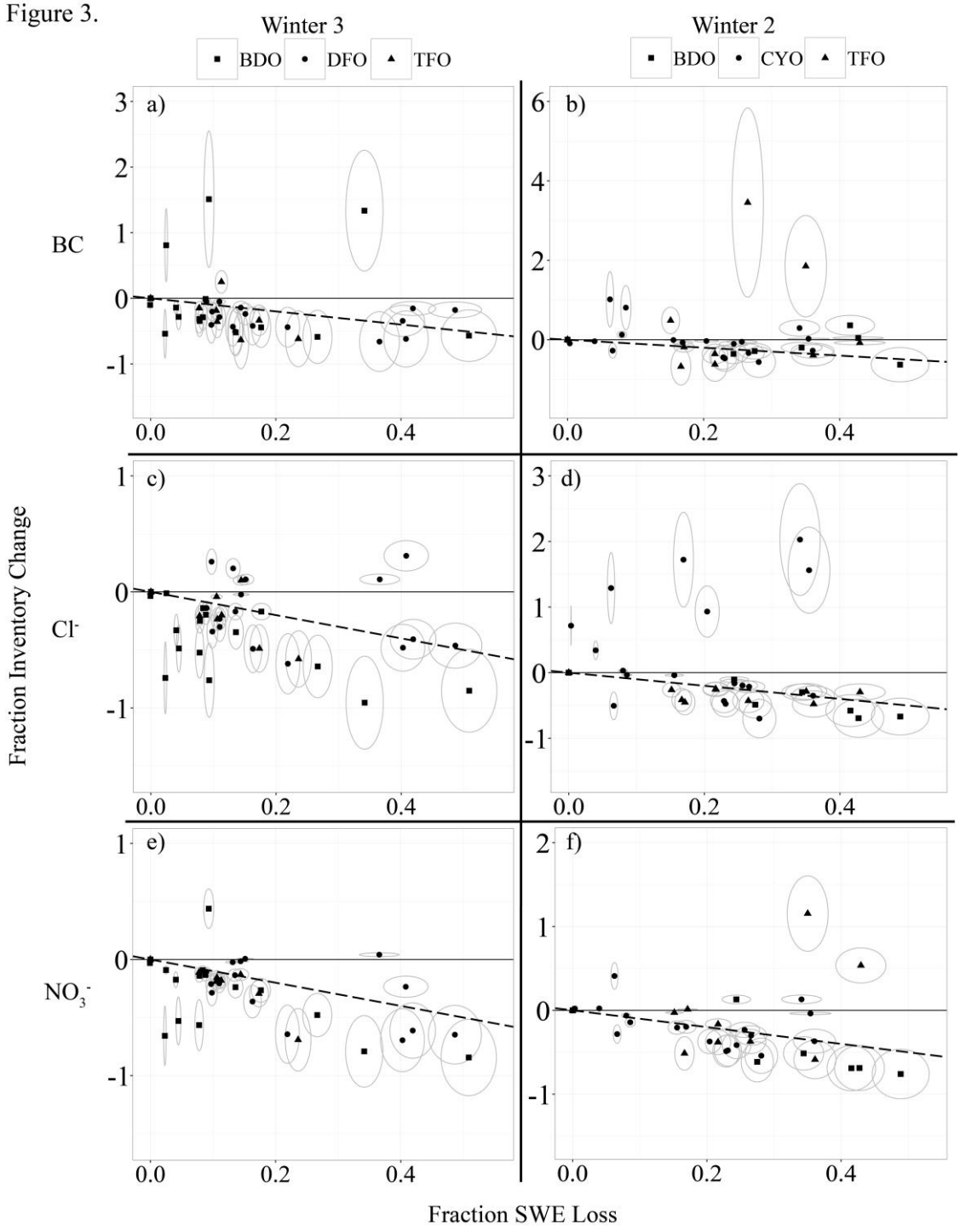

Figure 3. Daily BC loss (a and b), Cl^- loss (c and d), and NO_3^- loss (e and f) at all sites during the first fraction of melt in Winters Three and Two. Sites are denoted by symbol in the legend at the top of the plot. The dashed line (y = -x) indicates 1:-1 SWE loss to impurity inventory loss. The line at y=0 indicates steady impurity inventory during SWE loss. Instrument error and spatial variability are denoted by the ellipse drawn around each data point.

Figure 4.

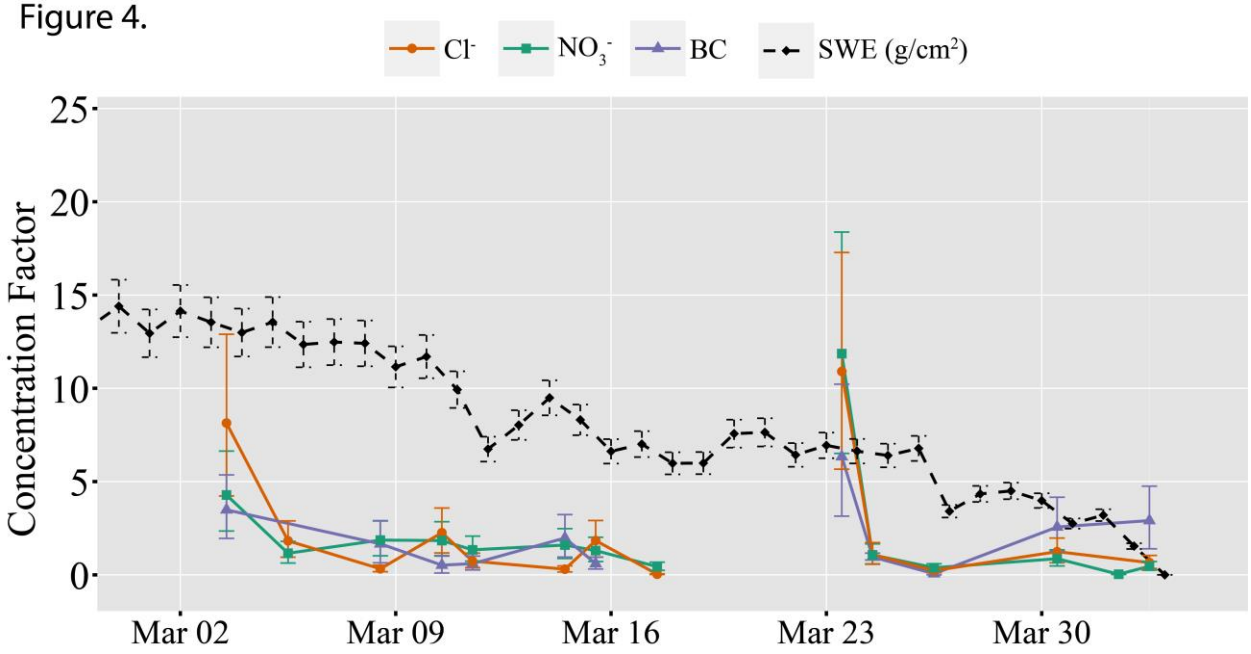

Figure 4. Concentration factor (CF) of snowpack meltwater over time for March of Winter 3 at BDO. Error bars include spatial variability and instrument error. The two separate melt events beginning on Mar 3 and Mar 23 best replicate the ionic pulse observed in laboratory settings, where the highest meltwater concentration is at the onset of melt. Note that calculated BC meltwater concentrations are also highest at the onset of melt events, with CF of ~3 and ~7 for the first and second event, respectively. CF is not continuous due and increase in smoothed SWE calculated in between records (see 2.5.3).

Figure 5.

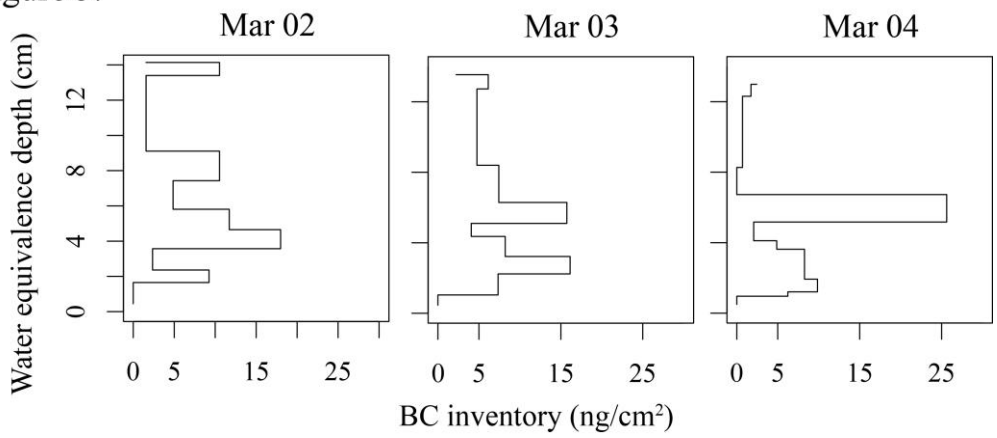

Figure 5. BC inventory on the day before snowmelt (Mar 2) to the day after the start of melt (Mar 4) at BDO in Winter 3 plotted against water equivalence depth. Inventory at the top of the snowpack decreases, while inventory at mid and lower depths increases.

Figure 6.

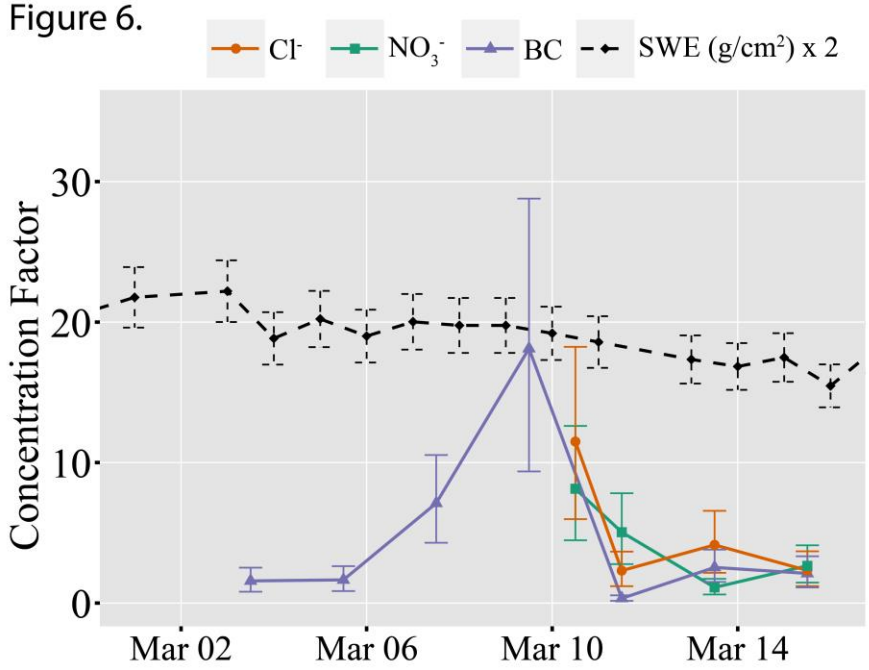

Figure 6. Concentration factor (Cf) of snowpack meltwater over time for early to mid-March in Winter 3 at DFO. Error bars include spatial variability and instrument error. SWE is scaled by a factor of 2 for clarity.

Figure 7.

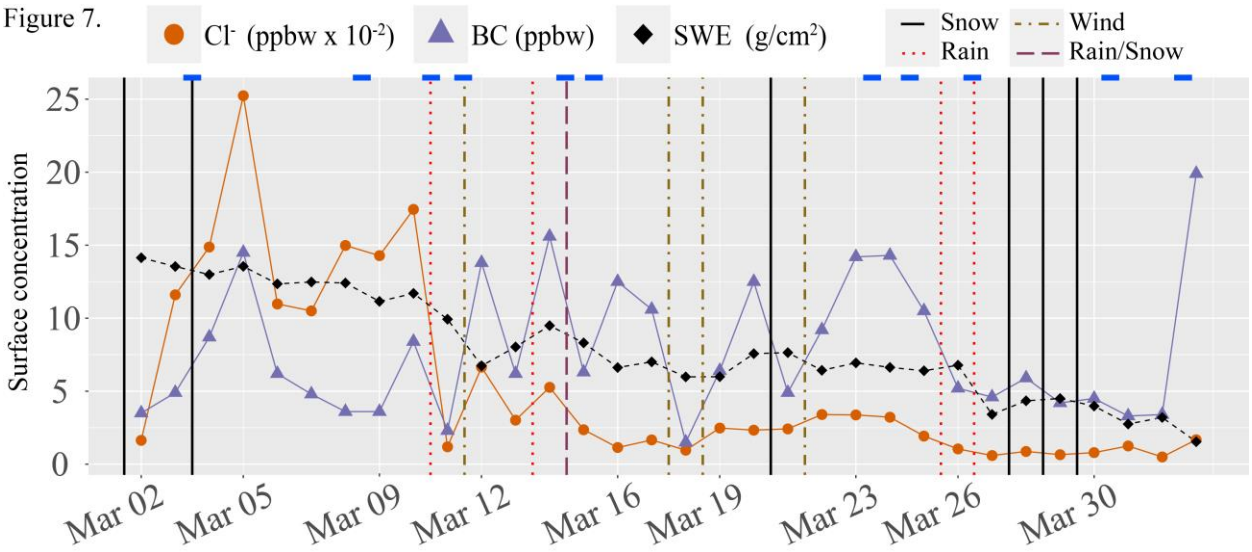

Figure 7. Snow water equivalence and surface concentrations for Cl^- and BC during last month of Winter 3 sampling at BDO. Observed snowfall is marked by the black solid line, rain fall by the red dotted line, excessive wind by the dark yellow dot-dash line, and rain/snow mix by the long dash line. Blue marks at the top of the plot indicate when integrated BC inventory and SWE are decreasing. Error bars have been excluded for clarity.

REFERENCES CITED

Aamaas, B., C. E. Bøggild, F. Stordal, T Berntsen, K. Holmen, and J. Ström (2011), Elemental carbon deposition to Svalbard snow from Norwegian settlements and long-range transport, Tellus B, 63, 340-351, doi:10.1111/j.1600-0889.2011.00531.x

Adolph, A., (in revision), Dominance of grain size impacts on seasonal snow albedo at deforested sites in New Hampshire, companion paper

Bales, R., R. Davis, and D. Stanley (1989), Ion elution through shallow homogeneous snow, Water Resources Research, 25(8), 1869–1877, doi:10.1029/WR025i008p01869

Bock, J. and H.-W. Jacobi (2010), Development of a Mechanism for Nitrate Photochemistry in Snow, J. Phys. Chem. A, 114, 1790-1796, doi:10.1021/jp909205e

Bond, T C., S. J. Doherty, D. W. Fahey, P. M. Forster, T. Berntsen, B. J. Deangelo, M. G. Flanner, S. Ghan, B. Kärcher, D. Koch, S. Kinne, Y. Kondo, and P. K. Quinn (2013), Bounding the role of black carbon in the climate system: A scientific assessment, J. Geophys. Res. Atmos., 118(11), 5380–5552, doi:10.1002/jgrd.50171

Box, J. E. and K. Steffen (2001), Sublimation on the Greenland Ice Sheet from automated weather station observations, J. Geophys. Res., 106(D24), 33965–33981, doi:10.1029/2001JD900219

Colbeck, S. C. (1981), A simulation of the enrichment of atmospheric pollutants in snow cover runoff, Water Resources Research, 17(5), 1383–1388, doi:10.1029/WR017i005p01383

Colbeck, S. C. (1979), Water Flow Through Heterogeneous Snow, Cold Regions Science and Technology, 1, 37–45, doi:10.1016/0165-232X(79)90017-X

Conway, H., A. Gades, and C. F. Raymond (1996), Albedo of dirty snow during conditions of melt, Water Resour. Res., 32(6), 1713–1718, doi:10.1029/96WR00712

Dibb, J. E., S. I. Whitlow, and M. Arsenault, (2007), Seasonal variations in the soluble ion content of snow at Summit. Greenland: Constraints from three years of daily surface snow samples. Atmospheric Environment, 41(24), 5007–5019, doi:10.1016/j.atmosenv.2006.12.010

Dibb, J. E., and J.-L. Jaffrezo (1997), Air-snow exchange investigations at Summit, Greenland: An overview, J. Geophys. Res., 102(C12), 26795–26807, doi:10.1029/96JC02303

Doherty, S. J., D. A. Hegg, J. E. Johnson, P. K. Quinn, J. P. Schwarz, C. Dang, and S. G. Warren (2016), Causes of variability in light absorption by particles in snow at sites in Idaho and Utah, J. Geophys. Res. Atmos., 121, 4751-4768, doi:10.1002/2015JD024375

Doherty, S. J., C. Dang, D. A. Hegg, R. Zhang, and S.G. Warren (2014), Black carbon and other light absorbing particles in snow of central North America, J Geophys. Res. Atmos., 119, 12,807-12,831, doi:10.1002/2014JD022350

Doherty, S. J., T. C. Grenfell, S. Forsström, D. L. Hegg, R. E. Brandt, and S. G. Warren (2013), Observed vertical redistribution of black carbon and other insoluble light-absorbing particles in melting snow, J. Geophys. Res. Atmos., 118(11), 5553–5569, doi:10.1002/jgrd.50235

Doherty, S. J., S. G. Warren, T. C. Grenfell, A. D. Clarke, and R. E. Brandt (2010), Light-absorbing impurities in Arctic snow, Atmos. Chem. Phys., 10, 11647-11680, doi:10.5194/acp-10-11647-2010

Feng, X., J. W. Kirchner, C. E. Renshaw, R. S. Osterhuber, B. Klaue, and S. Taylor (2001), A study of solute transport mechanisms using rare earth element tracers and artificial rainstorms on snow, Water Resour. Res., 37(5), 1425–1435, doi:10.1029/2000WR900376

Finamore, A (2013), It's Cold Outside: Winter Heating in New Hampshire, New Hampshire Employment Security, Economic and Labor Market Information Bureau, New Hampshire, USA

Flanner, M. G., C. S. Zender, J. T. Randerson, and P. J. Rasch (2007), Present-day climate forcing and response from black carbon in snow, J. Geophys. Res., 112, D11202, doi:10.1029/2006JD008003

Gustafsson, M. E. R. and L. G. Franzén (1999), Inland transport of marine aerosols in southern Sweden, Atmospheric Environment, 34, 313-325, doi:10.1016/S1352-2310(99)00198-3

Hadley, O. L., C. E. Corrigan, T. W. Kirchstetter, S. S. Cliff, and V. Ramanathan, (2010), Measured black carbon deposition on the Sierra Nevada snow pack and implication for snow pack retreat, Atmospheric Chemistry and Physics, 10, 7505–7513, doi:10.5194/acp-10-7505-2010

Hansen, J. and L. Nazarenko (2004), Soot climate forcing via snow and ice albedos, Proc. Natl. Acad. Sci. USA, 101(2), 423–428, doi:10.1073/ pnas.2237157100

Harrington, R. and R. C. Bales (1998a), Modeling ionic solute transport in melting snow, Water Resour. Res., 34(7), 1727–1736, doi:10.1029/98WR00557

Harrington, R. and R. C. Bales (1998b), Interannual, seasonal, and spatial patterns of meltwater and solute fluxes in a seasonal snowpack, Water Resour. Res., 34(4), 823–831, doi:10.1029/97WR03469

Hart, V. J. (1997), Spatial variability of soluble ions in surface and preserved snow at Summit, Greenland, M.S. thesis, Dep. of Earth Sciences, Univ. of New Hampshire, Durham, NH, USA

Hibberd, S. (1984), A model for pollutant concentrations during snow-melt, Journal of Glaciology, 30(104), 58-65

Johannessen, M. and A. Henriksen, (1978), Chemistry of snow meltwater: changes in concentration during melting. Water Resources Research, 14(4), 615–619, doi:10.1029/WR014i004p00615

Johannessen, M, T. Dale, and E. Gjessing, (1976), Acid precipitation in Norway: the regional distribution of contaminants in snow and the chemical concentration processes during snowmelt, International Association of Hydrological Sciences, 11(118), 116–120

Kaspari, S. D., M. Schwikowski, M. Gysel, M. G. Flanner, K. Shichang, S. Hou, and P. A. Mayewski (2011), Recent increase in black carbon concentrations from a Mt. Everest ice core spanning 1860-2000 AD, Geophysical Research Letters, 38, L04703, doi:10.1029/2010GL046096

Kuhn, M. (2001), The nutrient cycle through snow and ice, a review, Aquatic Sciences, 63(2), 150–167, doi:10.1007/PL00001348

Laborde, M., P. Mertes, P. Zieger, J. Dommen, U. Baltensperger, and M. Gysel (2012), Sensitivity of the Single Particle Soot Photometer to different black carbon types, Atmos. Meas. Tech., 5, 1031-1043, doi:10.5194/amt-5-1031-2012

Lee, J., V. E. Nez, X. Feng, J. W. Kirchner, R. Osterhuber, and C. E. Renshaw (2008), A study of solute redistribution and transport in seasonal snowpack using natural and artificial tracers, Journal of Hydrology, 357(3-4), 243–254, doi:10.1016/j.jhydrol.2008.05.004

Liang, B., J. Lehmann, D. Solomon, J. Kinyangi, J. Grossman, B. O'Neill, J. O. Skjemstad, J. Thies, F. J. Luizão, J. Petersen, and E. G. Neves, (2006), Black Carbon Increases Cation Exchange Capacity in Soils, Soil Science Society of America Journal, 70, 1719-1730, doi:10.2136/sssaj2005.0383

Liang, T., M. Chamecki, X. Yu (2016), Sea salt aerosol deposition in the coastal zone: A large eddy simulation study, Atmospheric Research, 180, 119-127, doi:10.1016/j.atmosres.2016.05.019

Lundmark, A. and B. Olofsson, (2007), Chloride deposition and distribution in soils along a deiced highway - Assessment using different methods of measurement, Water, Air, and Soil Pollution, 182(1-4), 173–185, doi:10.1007/s11270-006-9330-8

Meinander, O., S. Kazadzis, A. Arola, A. Riihela, P. Raisanen, R. Kivi, A. Kontu, R. Kouznetsov, M. Sofiev, J. Svensson, H. Soukanerva, V. Aaltonen, T. Manninen, J.-L. Roujean, and O. Hautecoeur (2013), Spectral albedo of seasonal snow during intensive melt period at Sodankylä, beyond the Arctic Circle, Atmospheric Chemistry and Physics, (13), 3793–3810, doi:10.5194/acp-13-3793-2013

Myhre, G., D. Shindell, F.-M. Bréon, W. Collins, J. Fuglestvedt, J. Huang, D. Koch, J.-F. Lamarque, D. Lee, B. Mendoza, T. Nakajima, A. Robock, G. Stephens, T. Takemura, and H. Zhang, (2013), Athropogenic and Natural Radiative Forcing, Climate Change 2013: The Physical Science Basis, Contribution of Working Group I to the Fifth Assessment Report of the Intergovernmental Panel on Climate Change [Stocker, T. F., D. Qin, G.-K. Plattner, M. Tignor, S. K. Allen, J. Boschung, A. Nauels, Y. Xia, V. Bex, and P. M. Midgley (eds.)], Cambridge University Press, Cambridge, United Kingdom and New York, NY, USA

Ogren, J. A., R. J. Charlson, and P. J. Groblicki (1983), Determination of Elemental Carbon in Rainwater, Anal. Chem, 55, 1569-1572, doi:10.1021/ac00260a027

Ohata, S., N. Moteki, J. Schwarz, D. Fahey, and Y. Kondo (2013), Evaluation of a Method to Measure Black Carbon Particles Suspended in Rainwater and Snow Samples, Aerosol Science and Technology, 47, 1073-1082, doi:10.1080/02786826.2013.824067

Oliver, B., J. B. Milne, and N. LaBarre (1974), Chloride and Lead in Urban Snow, Water Pollution Control Federation, 46, 4, 766-771

Polashenski, C. M., J. E. Dibb, M. G. Flanner, J. Y. Chen, Z. R. Courville, A. M. Lai, J. J. Schauer, M. M. Shafer, and M. Bergin (2015), Neither dust nor black carbon causing apparent albedo decline in Greenland's dry snow zone: Implications for MODIS C5 surface reflectance, Geophys. Res. Lett., 42(21), 9319–9327, doi:10.1002/2015GL065912

Qian, Y., H. Wang, R. Zhang, M. G. Flanner, and P. J. Rasch (2014), A sensitivity study on modeling black carbon in snow and its radiative forcing over the Arctic and Northern China, Environ. Res. Lett, 9, doi:10.1088/1748-9326/9/6/064001

Satoh, F., M. Nomura, H. Masumoto, D. Ashiya, and K. Sasa, (1999), Ionic elution from the acidic snowpack during spring thaw period in the northern part of Hokkaido, Research Bulletin of Hokkaido University Forests, 56(2), 1–10

Schwarz, J.P., R. S. Gao, A. E. Perring, J. R. Spackman., and D. W. Fahey (2013), Black carbon aerosol size in snow, Scientific Reports, 3, 1356, doi:10.1038/srep01356

Schwarz, J.P., S. J. Doherty, F. Li, S. T. Ruggiero, C. E. Tanner, A. E. Perring, R. S. Gao, and D. W. Fahey (2012), Assessing Single Particle Soot Photometer and Integrating Sphere/Integrating Sandwich Spectrophotometer measurement techniques for quantifying black carbon concentration in snow, Atmos. Meas. Tech., 5, 2581-2592, doi:10.5194/amt-5-2581-2012

Schwarz, J. P., R. S. Gao, D. W. Fahey, D. S. Thomson, L. A. Watts, J. C. Wilson, J. M. Reeves, M. Darbeheshti, D. G. Baumgardner, G. L. Kok, S. H. Chung, M. Schulz, J. Hendricks, A. Lauer, B. Ka, and J. G. Slowik (2006), Single-particle measurements of mid-latitude black carbon and light-scattering aerosols from the boundary layer to the lower stratosphere, Journal of Geophysical Research, 111(D16), 1–15, doi:10.1029/2006JD007076

Sergides, C. A., J. A. Jassim, A. R. Chughtai, and D. M. Smith (1987), The Structure of Hexane Soot. Part III: Ozonation Studies, Applied Spectroscopy, 41(3), 248-258, doi:10.1366/000370287448805

Sterle, K. M., J. R. McConnell, J. Dozier, R. Edwards, and M. G. Flanner (2013), Retention and radiative forcing of black carbon in eastern Sierra Nevada snow, The Cryosphere, 7, 365–374, doi:10.5194/tc-7-365-2013

Svensson, J., J. Ström, M. Hansson, H. Lihavainen, and V.-M. Kerminen (2013), Observed metre scale horizontal variability of elemental carbon in surface snow, Environmental Research Letters, 8(3), 034012, doi:10.1088/1748-9326/8/3/034012

Tedesco, M., S. Doherty, X. Fettweis, P. Alexander, J. Jeyaratnam, and J. Stroeve (2016), The darkening of the Greenland ice sheet: trends, drivers, and projections (1981–2100), The Cryosphere, 10, 477–496, doi:10.5194/tc-10-477-2016

Tukey, J (1977), Exploratory Data Analysis, Addison-Wesley, Boston, Massachusetts, 43-44

Ulrich, J (2015), TTR: Technical Trading Rules, R package version 0.23-0, CRAN.R-TTR

U.S. EPA (2009), Final Report: Integrated Science Assessment for Particulate Matter, U.S. Environmental Protection Agency, Washington, DC, EPA/600/R-08/139F

Williams, M. W., C. Seibold, and K. Chowanski (2009), Storage and release of solutes from a subalpine seasonal snowpack: soil and stream water response, Niwot Ridge, Colorado, Biogeochemistry, 95(1), 77–94, doi:10.1007/s10533-009-9288-x

Williams, M. W., and J. M. Melack (1991), Solute chemistry of snowmelt and runoff in an Alpine Basin, Sierra Nevada, Water Resour. Res., 27(7), 1575–1588, doi:10.1029/90WR02774

Wendl, I. A., J. A. Menking, R. Färber, M. Gysel, S. D. Kaspari, M. J. G. Laborde, and M. Schwikowski (2014), Optimized method for black carbon analysis in ice and snow using the Single Particle Soot Photometer, Atmos. Meas. Tech., 7, 2667-2681, doi:10.5194/amt-7-2667-2014

APPENDIX

The data generated for this research and other data collected through NH EPSCoR can be found on the Data Discovery Center at https://ddc.unh.edu/ddc_data/variables/list/.